

A mathematical model for carbothermic nitridation of carbon/metal oxide pellet—effect of pressure gradient

H. K. CHEN*

Department of Chemical Engineering, Hwa Hsia College of Technology and Commerce, Taipei, Taiwan 235

C. I. LIN

Department of Chemical Engineering, National Taiwan University of Science and Technology, Taipei, Taiwan 106

A mathematical model has been proposed for describing the carbothermic nitridation of carbon/metal oxide pellet in a stream of nitrogen. Based on the model, dimensionless governing equations were derived to represent the non-isobaric system. Effects of the following five parameters on the conversion of solid C and yield of solid E have been found to be similar to that of an isobaric system: the reaction/diffusion ratio σ^2 , the reactivity ratios β_1 and β_2 , the reactant amount ratio γ and the Sherwood number N_{Sh} . The reaction rate was found to be high when the value of a dimensionless viscous constant B^* was large. The reaction rate for the non-isobaric system was generally found to be lower than that for the isobaric system. © 1999 Kluwer Academic Publishers

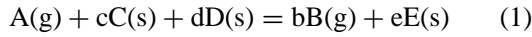
Nomenclature

A, B	symbols for A and B, respectively [-]	P_{Ab}, P_{Bb}	partial pressures of A and B in bulk gas, respectively [atm]
B_o	viscous constant [m ²]	P_t	total pressure [atm]
B^*	dimensionless viscous constant defined in Table II [-]	R	gas constant [atm·m ³ /(kmol·K)]
b, c, d, e	stoichiometric number [-]	t	reaction time [s]
C, D, E	symbols for C, D and E, respectively [-]	t^*	dimensionless time defined in Table II [-]
C_C, C_D, C_E	concentrations of solids C, D and E, respectively [kmol/m ³]	T	reaction temperature [K]
C_{Co}, C_{Do}, C_{Eo}	initial concentration of solids C, D and E, respectively [kmol/m ³]	X_C, X_D	conversions of solids C and D, respectively [-]
D_{eKA}	effective Knudsen diffusivity of gases A [m ² /s]	Y_E	yield of solid E [-]
d_C, d_D	grain sizes of C and D, respectively [m]	z	coordinate [m]
h	mass transfer coefficient [kmol/(s·m ² ·atm)]	β_1, β_2	reactivity ratios defined in Table II [-]
L	half-thickness of solid matrix [m]	γ	reactant amount ratio defined in Table II [-]
l_1, l_2, \dots, l_8	reaction order [-]	η	dimensionless coordinate defined in Table II [-]
m_1, m_2, \dots, m_8	reaction order [-]	ξ_C, ξ_D, ξ_E	dimensionless concentrations of solids C, D and E defined in Table II, respectively [-]
N_A, N_B	fluxes of gases A and B, respectively [kmol/(s·m ²)]	ρ_o	initial bulk density [kg/m ³]
\tilde{N}_A, \tilde{N}_B	dimensionless fluxes of gases A and B defined in Table II, respectively [-]	σ^2	reaction/diffusion ratio defined in Table II [-]
N_{Sh}	Sherwood number [-]	φ_A, φ_B	dimensionless concentrations of gases A and B defined in Table II, respectively [-]
n_1, n_2, \dots, n_8	reaction order [-]	$\varphi_{Ab}, \varphi_{Bb}$	dimensionless concentrations of gases A and B in the bulk phase defined in Table II, respectively [-]
P_A, P_B	partial pressures of A and B, respectively [atm]		

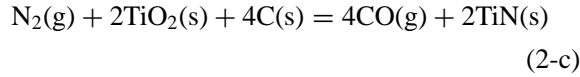
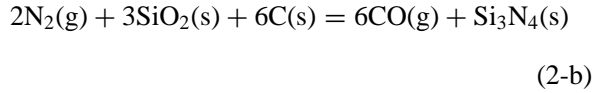
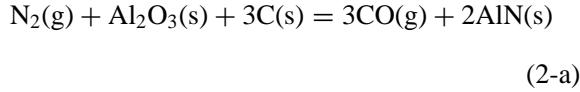
* Correspondence concerning this article should be addressed to H. K. Chen.

1. Introduction

A gas-solid reaction of the following type



is normally found in the carbothermic nitridation of aluminium oxide, silicon oxide and titanium oxide:



Most reports [1–3, 7–9] of this kind of gas-solid reaction have been experimental. We previously proposed a mathematical model [4] to interpret the experimental results of the system of carbothermic nitridation of aluminium oxide. Later, a general mathematical model [5] was suggested to interpret the nitridation of carbon/metal oxide powder mixture. Gas pore diffusion was assumed to have a normal diffusion region in these two papers. Subsequently, a mathematical model for an isobaric system with Knudsen diffusion was proposed [6]. If the solid pellet of carbon/metal oxide is sufficiently thin, the system can be assumed to be isobaric. However, when the pellet is thick the isobaric assumption should be discarded, i.e. the effect of pressure gradient should be considered. However, a mathematical model taking this factor into account has not yet been found. Therefore, this work is to develop a physico-chemical model for the Knudsen diffusion region which can be applied to the non-isobaric system. The effects of reaction/diffusion ratio, reactivity ratios, reactant amount ratio, Sherwood number and dimensionless viscous constant on the conversion of solid C and yield of solid E are studied in this investigation. A comparison of the reaction rates for the isobaric and non-isobaric cases is made.

2. Mathematical model

A slab-like pellet made up of uniformly mixed solid grains consisting of species C and D is considered here. Solids C and D react with gas A according to reaction (1). Gas A is present in the bulk gas.

The following assumptions are made:

- 1) The system is isothermal.
- 2) Pellet structure does not change during reaction.
- 3) The pseudo-steady state assumption is applicable.
- 4) Gas diffusion in the pores is in the Knudsen diffusion region.
- 5) Mass transfer coefficients of gases A and B in the gas film are assumed to be the same.

Within the framework of the above assumptions, the problem may be stated by combining equations for

conservation of the gases with a mass balance for the solids. The results are expressed as

$$N_A = -(D_{eKA}/RT) \frac{dP_A}{dz} - P_A(B_o/\mu RT) \frac{dP_t}{dz} \quad (3)$$

$$P_B = P_t - P_A \quad (4)$$

$$\frac{dN_A}{dz} = -k_1 \exp(-E_1/RT) d_C^{n_1} d_D^{n_2} \rho_o^{n_3} C_C^{n_4} C_D^{n_5} C_E^{n_6} P_A^{n_7} P_B^{n_8} \quad (5)$$

$$\frac{dN_B}{dz} = bk_1 \exp(-E_1/RT) d_C^{n_1} d_D^{n_2} \rho_o^{n_3} C_C^{n_4} C_D^{n_5} C_E^{n_6} P_A^{n_7} P_B^{n_8} \quad (6)$$

The meanings of all symbols can be found in the Nomenclature Section. D_{eKA} is effective Knudsen diffusivity in which porosity and tortuosity have been taken into account. B_o is the viscous constant which correlates with the pore diameter in the solid sample, $B_o = d^2/32$. The pore diameter is d .

The conservation of reactants C and D, together with product E may be written as follows.

$$\frac{\partial C_C}{\partial t} = -k_1 \exp(-E_1/RT) d_C^{n_1} d_D^{n_2} \rho_o^{n_3} C_C^{n_4} C_D^{n_5} C_E^{n_6} P_A^{n_7} P_B^{n_8} \quad (7)$$

$$\frac{\partial C_D}{\partial t} = -k_2 \exp(-E_2/RT) d_C^{m_1} d_D^{m_2} \rho_o^{m_3} C_C^{m_4} C_D^{m_5} C_E^{m_6} P_A^{m_7} P_B^{m_8} \quad (8)$$

$$\frac{\partial C_E}{\partial t} = k_3 \exp(-E_3/RT) d_C^{l_1} d_D^{l_2} \rho_o^{l_3} C_C^{l_4} C_D^{l_5} C_E^{l_6} P_A^{l_7} P_B^{l_8} \quad (9)$$

Initially, the concentrations of solids C, D and E are expressed as

$$C_C = C_{C_0} \quad \text{at } t = 0 \quad (10-a)$$

$$C_D = C_{D_0} \quad \text{at } t = 0 \quad (10-b)$$

$$C_E = 0 \quad \text{at } t = 0 \quad (10-c)$$

Due to symmetry, the boundary conditions at the center of the pellet can be written as

$$N_A = 0 \quad \text{at } z = 0 \quad (11-a)$$

$$N_B = 0 \quad \text{at } z = 0 \quad (11-b)$$

On the surface of the pellet, the fluxes of gases transferred through the boundary layer are equal to the fluxes diffused through the pellet. Thus, we have

$$N_A = h(P_A - P_{Ab}) \quad \text{at } z = L \quad (12-a)$$

$$N_B = h(P_B - P_{Bb}) \quad \text{at } z = L \quad (12-b)$$

If resistance to mass transfer in the gas film is neglected, the partial pressures of component gases on the pellet

TABLE I Dimensionless governing equations, initial conditions and boundary conditions

Governing equations:		
$-\tilde{N}_A = (1 + B^* \varphi_A) \frac{d\varphi_A}{d\eta} + B^* \varphi_A \frac{d\varphi_B}{d\eta}$	(14)	
$\varphi_B = 1 - \varphi_A$	(15)	
$\frac{d\tilde{N}_A}{d\eta} = -\sigma^2 \beta_2 \xi_C^{n_4} \xi_D^{n_5} \xi_E^{n_6} \varphi_A^{n_7} \varphi_B^{n_8}$	(16)	
$\frac{d\tilde{N}_B}{d\eta} = b\sigma^2 \beta_1 \xi_C^{n_4} \xi_D^{n_5} \xi_E^{n_6} \varphi_A^{n_7} \varphi_B^{n_8}$	(17)	
$\frac{\partial \xi_C}{\partial t^*} = -\xi_C^{m_4} \xi_D^{m_5} \xi_E^{m_6} \varphi_A^{m_7} \varphi_B^{m_8}$	(18)	
$\frac{\partial \xi_D}{\partial t^*} = -\beta_1 \xi_C^{m_4} \xi_D^{m_5} \xi_E^{m_6} \varphi_A^{m_7} \varphi_B^{m_8}$	(19)	
$\frac{\partial \xi_E}{\partial t^*} = \beta_2 \xi_C^{l_4} \xi_D^{l_5} \xi_E^{l_6} \varphi_A^{l_7} \varphi_B^{l_8}$	(20)	
Initial conditions:		
$\xi_C = 1$	at $t^* = 0$	(21-a)
$\xi_D = \gamma$	at $t^* = 0$	(21-b)
$\xi_E = 0$	at $t^* = 0$	(21-c)
Boundary conditions:		
$\tilde{N}_A = 0, \tilde{N}_B = 0$	at $\eta = 0$	(22-a)
$\tilde{N}_A = N_{Sh}(\varphi_A - \varphi_{Ab})$ or $\varphi_A = \varphi_{Ab}$	at $\eta = 1$	(22-b)
$\tilde{N}_B = N_{Sh}(\varphi_B - \varphi_{Bb})$ or $\varphi_B = \varphi_{Bb}$	at $\eta = 1$	(22-c)

surface are equal to those in the bulk gas. The boundary conditions of Equations 12a and b can therefore be replaced by

$$P_A = P_{Ab} \quad \text{at } z = L \quad (13-a)$$

$$P_B = P_{Bb} \quad \text{at } z = L \quad (13-b)$$

To facilitate the analysis, Equations 3 through 13 are transformed into dimensionless forms, as shown in Table I. The definitions of the dimensionless quantities are listed in Table II.

The conversions of solids C and D and the yield of solid E are calculated according to the following equations

$$X_C = \int_0^1 (1 - \xi_C) d\eta \quad (40)$$

$$X_D = \int_0^1 (\gamma - \xi_D) d\eta \quad (41)$$

$$Y_E = \int_0^1 \xi_E d\eta \quad (42)$$

The numerical method needed to obtain the solution is the same as that described by Chen and Lin [4–6], except that in the present case their two equations of the boundary-value problem are replaced by four, Equations 3 through 6.

3. Results and discussion

The values of stoichiometric numbers and pertinent parameters employed for the calculation are listed in Table III, with the stoichiometric numbers corresponding to the carbothermic nitridation of

TABLE II Definitions of dimensionless quantities

Gas concentrations:	
$\varphi_A = P_A/P_t$	(23)
$\varphi_B = P_B/P_t$	(24)
Gas concentration in the bulk phase:	
$\varphi_{Ab} = P_{Ab}/P_t$	(25)
$\varphi_{Bb} = P_{Bb}/P_t$	(26)
Diffusion flux:	
$\tilde{N}_A = (N_A LRT)/(P_t D_{eKA})$	(27)
$\tilde{N}_B = (N_B LRT)/(P_t D_{eKA})$	(28)
Solid concentrations:	
$\xi_C = C_C/C_{C0}$	(29)
$\xi_D = C_D/C_{D0}$	(30)
$\xi_E = C_E/C_{C0}$	(31)
Coordinate:	
$\eta = z/L$	(32)
Time:	
$t^* = k_1 t/C_{C0}$	(33)
Reaction/diffusion ratio:	
$\sigma^2 = (L^2 RT k_1)/(P_t D_{eKA})$	(34)
Reactivity ratio:	
$\beta_1 = k_2/k_1$	(35)
$\beta_2 = k_3/k_1$	(36)
Reactant amount ratio:	
$\gamma = C_{D0}/C_{C0}$	(37)
Dimensionless viscous constant	
$B^* = (B_0 P_t)/(\mu D_{eKA})$	(38)
Sherwood number	
$N_{Sh} = hL/D_{eKA}$	(39)

TABLE III Values of stoichiometric number and pertinent parameters

Stoichiometric number or parameter	Value
b	3.0
c	1.0
d	3.0
e	2.0
n ₄	2.1
n ₅	1.1
n ₆	-0.48
n ₇	0.95
n ₈	0.01
m ₄	0.94
m ₅	1.65
m ₆	-0.58
m ₇	0.87
m ₈	0.01
l ₄	0.45
l ₅	0.35
l ₆	0.16
l ₇	0.94
l ₈	0.01

C/Al₂O₃. The values of parameters employed are obtained from experimental data of this reaction system [2]. The only difference between the governing equations of the non-isobaric system and the isobaric system is the form of the diffusion equation, Equation 3, of this paper for the non-isobaric system and Equation 2 in [6] for the isobaric system. The other equations, initial conditions and boundary conditions are exactly the same. The effects of five parameters, namely, reaction/diffusion ratio σ^2 , reactivity ratios, β_1 and β_2 , reactant amount ratio, γ and Sherwood number N_{Sh} on the conversion of solid C and the yield of product E are similar in the non-isobaric and isobaric

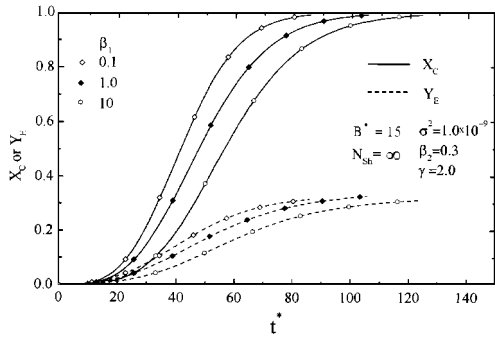


Figure 1 Plot of conversion of solid C, X_C and yield of solid E, Y_E against dimensionless time. The effect of β_1 .

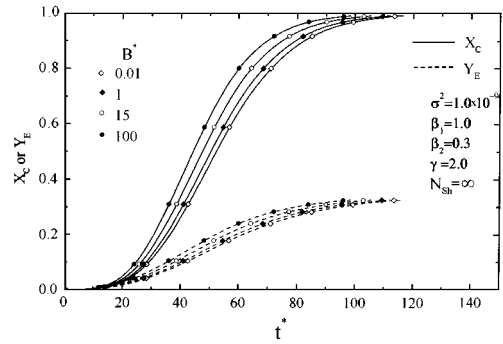


Figure 4 Plot of conversion of solid C, X_C and yield of solid E, Y_E against dimensionless time. The effect of B^* .

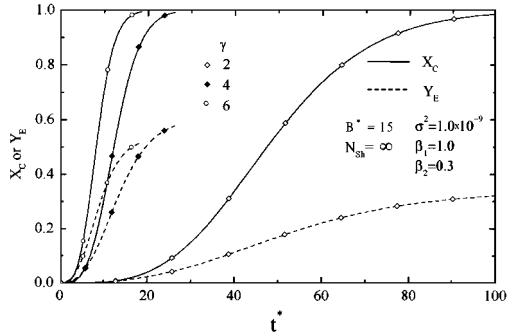


Figure 2 Plot of conversion of solid C, X_C and yield of solid E, Y_E against dimensionless time. The effect of γ .

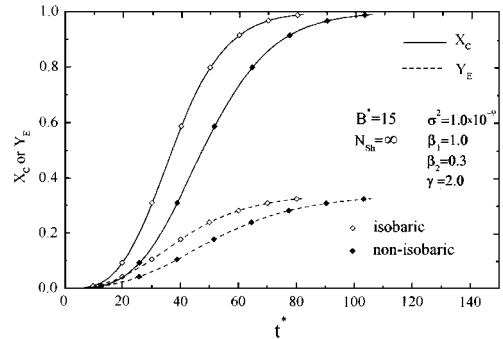


Figure 5 Plot of conversion of solid C, X_C and yield of solid E, Y_E against dimensionless time. Comparison of non-isobaric case and isobaric case.

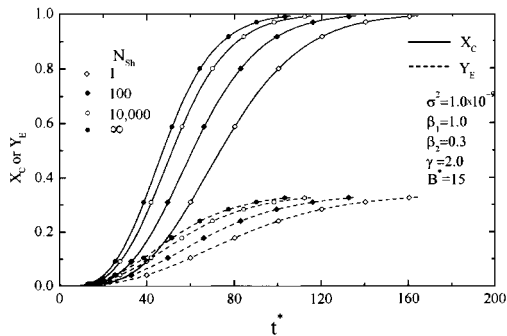


Figure 3 Plot of conversion of solid C, X_C and yield of solid E, Y_E against dimensionless time. The effect of N_{Sh} .

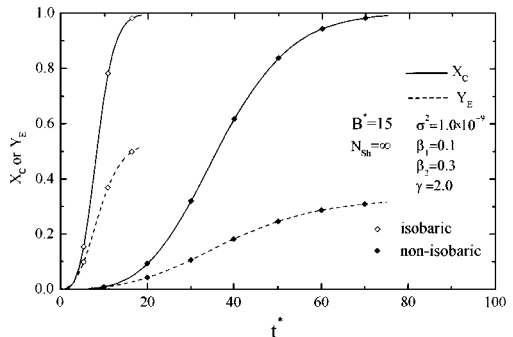


Figure 6 Plot of conversion of solid C, X_C and yield of solid E, Y_E against dimensionless time. Comparison of non-isobaric case and isobaric case.

systems. According to the results obtained, it is found that the reaction would increase when the values of β_2 , γ or N_{Sh} increased or the values of σ^2 or β_1 decreased. Figs 1–3 show some of the results obtained.

A larger value of B^* indicates a larger pore size in the solid sample. A larger pore size produces a high rate of diffusion of gas A into the solid sample, accelerating the reaction. The computed conversion curves (Fig. 4) confirm this viewpoint.

Figs 5–7 show the conversions of solid C, X_C together with the yields of solid E, Y_E against dimensionless time at different conditions. It is generally found that when the system is non-isobaric, the reaction is slower than under isobaric conditions. The mathematical model and calculations for the isobaric system is rather simple compared to those for the non-isobaric system. Hence, if the pellet is thin, the isobaric assumption is usually employed. However, if the pellet is thick, producing pressure gradient exists, the isobaric

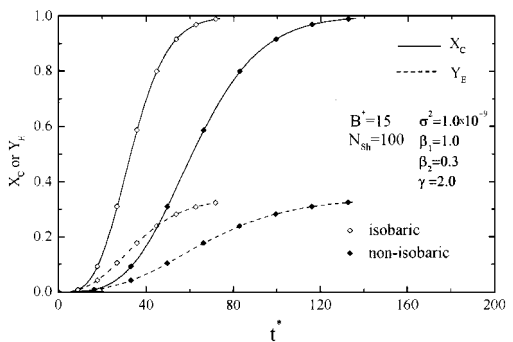


Figure 7 Plot of conversion of solid C, X_C and yield of solid E, Y_E against dimensionless time. Comparison of non-isobaric case and isobaric case.

assumption should be discarded to prevent the calculation errors.

4. Conclusions

1. The effects of five parameters, σ^2 , β_1 , β_2 , γ , N_{Sh} , on the conversion of solid C and yield of product E are similar in both non-isobaric and isobaric cases.

2. A larger value of B^* produces a higher rate of reaction.

3. Other conditions being equal, the rate of reaction of a non-isobaric case is lower than that for an isobaric case.

Acknowledgement

We thank the National Science Council of the Republic of China for financial support (Grant No. NSC86-2621-E-146-003-T).

References

1. H. INOUE, A. TSUNG and M. KASORI, *Journal of Materials Science* **25** (1990) 2359.
2. H. K. CHEN, C. I. LIN and C. LEE, *Journal of the American Ceramic Society* **77**(7) (1994) 1753.
3. H. K. CHEN and C. I. LIN, *Journal of the Chinese Institute of Chemical Engineers* **25**(5) (1994) 335.
4. H. K. CHEN and C. I. LIN, *Journal of Chemical Engineering of Japan* **7**(1) (1994) 90.
5. H. K. CHEN and C. I. LIN, *Journal of the Chinese Institute of Chemical Engineers* **25**(6) (1994) 35.
6. H. K. CHEN and C. I. LIN (submitted).
7. H. L. WANG, M. S. Thesis, Department of Mineral Metallurgy and Materials Science, National Cheng Kung University, Tainan, Taiwan (1988).
8. N. KURAMOTO and H. TANIGUCHI: U.S. Patent 45,618,592 (1986).
9. S. HIRAI, T. MIWA, M. OZAWA and H. G. KATAYAMA, *Journal of Japan Institute of Metals* **53**(10) (1989) 1035.

Received 13 March
and accepted 20 August 1998